Starlike Polymeric Architectures by Atom Transfer Radical Polymerization: Templates for the Production of Low Dielectric Constant Thin Films

Andreas Heise,[†,§] Cattien Nguyen,[†] Raouf Malek,[†] James L. Hedrick,*[,†] Curtis W. Frank,[‡] and Robert D. Miller*[,†]

IBM Almaden Research Center, 650 Harry Road, San Jose, California 95120, and Department of Chemical Engineering, Stanford University, Stanford, California 95305

Received July 7, 1999; Revised Manuscript Received January 17, 2000

ABSTRACT: The synthesis of novel poly(methyl methacrylate)s with starlike architectures by controlled radical polymerization starting from dendritic 2-, 4-, 6-, and 12-arm multifunctional initiators is described. The more highly functionalized initiators were obtained by coupling a bromo-functionalized bis-(hydroxymethyl)propionic acid (bis-MPA) first generation dendron to hydroxyl-functionalized precursors. The controlled free radical character of the atom transfer radical polymerization is supported by the remarkably low polydispersities of the polymers and the close correspondence between the calculated and measured molecular weights. NMR studies on the polymers were consistent with initiation occurring from all initiator arms for the 2-, 4-, and 6-arm derivatives. Initial studies on deuterated polymers derived from 12-arm initiator suggest that in some cases initiation was not quantitative. In addition, starlike random copolymers of methyl methacrylate containing varying amounts of hydroxyethyl methacrylate with slightly higher polydispersities have been synthesized. Preliminary results show that these copolymers can be used to produce nanophase-separated inorganic/organic hybrids by templating vitrification of methylsilsesquioxane (MSSQ) and nanoporous thin films after subsequent thermal degradation of the organic polymer. Transmission electron microscopy confirms a nanoporous morphology of the thin films, and a decrease of the dielectric constant is observed.

Introduction

It is well-known that not only the elemental composition but also the molecular arrangement of a molecule has a significant impact on the properties of the material. In organic chemistry, for example, this is reflected by the different properties of stereoisomers. For macromolecules, the effect of the molecular architecture and the shape on the resulting polymer properties has been clearly demonstrated for dendrimers and hyperbranched materials. For these materials, the molecular properties are clearly different from linear analogues.[1] In many respects, dendrimers represent a transition from small organic molecules to polymer chemistry; e.g., these materials, although polymeric in nature, combine a defined three-dimensional macromolecular architecture with very low polydispersities and are derived by a stepwise synthesis employing classical organic coupling reactions.[2−4] However, the tedious stepwise synthesis of most dendrimers limits their utilization in most technology applications. To overcome this drawback, scientists are currently focusing on controlled polymerization techniques for the preparation of globular high molecular weight materials. Accordingly, block, star,[5−12] and well-defined hyperbranched polymers[3,13−16] have been reported in the literature. However, until recently the lack of control in classical radical polymerization procedures has limited the application of this technique for the preparation of well-defined polymer architectures. This situation has changed dramatically recently due to the progress in controlled radical polymerization techniques, such as nitroxide-mediated,[17−24] transition metal-mediated atom transfer radical polymerization procedures (ATRP),[25−33] and dithio component-mediated reversible addition−fragmentation chain transfer (RAFT) polymerization.[34] These advances provide a simple pathway for the preparation of a wide variety of interesting polymers with well-defined structures. Architectural control in polymers is particularly important because of the pronounced effect on the polymer properties such as intrinsic viscosity,[6] T_g, polymer morphology, and interfacial activity in pure polymers and polymer blends.

To maintain performance as the field of microelectronics moves toward smaller devices, new advanced materials are required including low dielectric constant materials for on-chip insulating layers.[35] Currently, efforts are proceeding in the industry to replace or modify the conventional vapor-deposited silicon oxide (k = 3.9−4.2) for such applications. Our ultimate goal in this area is to lower the dielectric constant of spin-on silicate materials by the incorporation of controlled nanoporosity.[35−37] For the microelectronic applications envisioned for these nanoporous materials, it is essential to control the pore size and distribution as well as any interconnectivity between the pores. One route for introducing pores into a organosilicate matrix involves the preparation of molecular composites or nanophase-separated organic/inorganic hybrids made by blending suitably functionalized polymers into low molecular weight silsesquioxanes (SSQ). After templated vitrification of the SSQ matrix, the organic phase may be removed by thermal processing.

Branched polyesters derived from the ring-opening polymerization (ROP) of caprolactone and related derivatives with multifunctional initiators represent one

[†] IBM Almaden Research Center.
[‡] Stanford University.
[§] Current address: DSM Research, 6160 MD Geleen, The Netherlands.

10.1021/ma991091r CCC: $19.00
Published on Web 03/14/2000

type of thermally labile polymer used for templating porosity in organosilicates. When linear poly(caprolactone)s (PCL)s are mixed with various SSQ matrix materials, the thermal curing of the spin-coated films results in unacceptable macroscopic phase separation prior to the decomposition of the pore generators. On the other hand, optically clear nanoscopic hybrids can be produced from SSQ matrix materials and branched and dendritic PCL's. The control of the phase morphology in these hybrid systems was attributed in part to the stronger interactions of the organic polymer with the SSQ matrix prior to and during the templated vitrification due to the increased number of end groups and abundant polymer functionality. This coupled with the limited mobility and low chain entanglements characteristic of the branched architectures is believed to be responsible for the formation of controlled nanostructures. Nanoporous thin films with dielectric constants below 2.2 could be obtained by high-temperature processing.[38] These results, in comparison with the unsuccessful attempts to utilize linear PCL derivatives for such purposes, clearly demonstrate the utility of controlled macromolecular architectures.

We now extend this synthetic approach to the preparation of starlike PMMA homo- and copolymers produced by controlled radical polymerization techniques. Such polymers are potenially attractive candidates for the preparation of nanoporous polymers for many of the reasons discussed. In addition, the large number of commercially available monomers provides the opportunity to tailor the side chain functionalities to facilitate polymer−polymer compatibilization. The clean thermal degradation profiles of many MMA homo- and copolymers derived by ATRP[32] also validate their potential utility as pore generators (porogens) in the formation of porous organosilicates from the corresponding polymer hybrids.

Recently, we have reported the use of a dendritic atom transfer radical polymerization (ATRP) initiator for the synthesis of starlike PMMA homopolymers and random and block copolymers.[39−41] Utilizing monomers based on 2,2-bis(hydroxymethyl)propionic acid (bis-MPA) as building blocks, initiators with 12 arms or more can be prepared. The synthesis of starlike poly(styrene) and poly(methyl methacrylate) (PMMA) from multiarm calixarene-based initiators by ATRP processes has also recently been described, and star polymers with up to eight arms were reported.[42,43] Star polymers utilizing ATRP procedures have also recently been prepared by in an arm first approach.[44] Here we describe the synthesis of other multiarm initiators and discuss their use for atom transfer radical polymerization. Preliminary results suggest that materials of this type are useful for the formation of nanoporous organosilicate thin films.

Experimental Section

Materials and Methods. All chemicals were purchased from Aldrich Chemical Co. and used without any further purification unless otherwise noted. Methyl methacrylate was distilled from CaH_2 under reduced pressure. Hydroxyethyl methacrylate was distilled under reduced pressure using a short path distillation apparatus. Tetrahydrofuran was freshly distilled from potassium.

^{1}H NMR spectra were recorded in $CDCl_3$ solution on a Brucker AM 250 (250 MHz) spectrometer, with the solvent signal as an internal standard. ^{13}C NMR spectra were similarly recorded in $CDCl_3$ solution at 62.5 MHz on a Brucker AM 250 spectrometer with the solvent carbon signal serving as internal standard. Analytical TLC was performed on commercial Merck plates coated with silica gel GF_{254} (0.25 mm thick). Silica gel used for flash chromatography was Merck Kieselgel 60 (230−400 mesh). Size exclusion chromatography was carried out on a Waters chromatograph connected to a Waters 410 differential refractometer. Four 5 μm Waters columns (300 × 7.7 mm) connected in series in order of increasing pore size (100, 1000, 10^5, and 10^6 Å) were used with THF as eluant. Glass transition temperatures (T_g) were measured on a Perkin-Elmer DSC 7 instrument.

The spin-on films of methylsilsesquioxane (MSSQ) low molecular weight polymers were prepared as follows. MSSQ (M_n ∼950 g/mol as measured by GPC) in a solution containing 30% (w/w) of the polymers (based on MSSQ) in propylene glycol methyl ether acetate (PM-acetate) was loaded into a disposable syringe and passed through a 0.2 μm Acrodisc CR PTFE filter directly onto a polished, 1 in. silicon wafer. The wafer was spun at 2500 rpm for 30 s and placed directly onto a hot plate at 50 °C under house nitrogen. To cure the resin, the temperature was ramped to a desired set point (425 °C) over a 4 h period and held at this temperature for 2 h before cooling.

Polymer samples for IR spectroscopy were prepared on double side polished, 0.25° wedged, IR grade silicon wafers (purchased from Harrick Scientific Corp.). Other samples were studied either as thin films on NaCl crystals or in KBr pellets. IR spectra were obtained using a Nicolet Magna-IR spectrometer 550 coupled with Ominic Version 2.0 software at a resolution of 4 cm^{-1} and recording 16 scans per spectrum. Dielectric constant measurements were carried out with a Hewlett-Packard multifrequency LCR meter model 4275A interfaced with a personal computer using LABSPC software to collect data. Electrodes were connected via HP 16048A test leads. Silsesquioxane samples were spun as thin films (on glass substrates) and sandwiched between evaporated patterned Al electrodes. All samples were placed in a brass testing cell that included a thermocouple mounted at the sample and were heated in a nitrogen atmosphere from below using a hot plate and a Eurotherm temperature controller assembly. The heating rate in all cases was 5 °C/min, and data were collected upon heating from −100 to 150 °C.

The index of refraction of the films was measured with Metricon model 2010 prism coupler at 633 nm. Multiple measurements on different parts of the films were recorded to check for reproducibility.

Initiators. *Building Block **3***. 2-Bromo-2-methylpropionyl bromide **2** (44 mL, 357 mmol) was added dropwise to a solution of bis(hydroxymethyl)propionic acid (bis-MPA), **1** (20 g, 149 mmol, 298 equiv of OH), and triethylamine (52 mL, 366 mmol) in 500 mL of dry dichloromethane at 0 °C under argon atmosphere. After stirring at 0 °C for 1 h, the reaction was completed by stirring for another 2 h at 25 °C. After evaporation of the solvent, the residue was dissolved in diethyl ether, and the triethylamine hydrochloride was filtered off. The solution was then extracted with 2 N hydrochloride, the ether phase dried over $MgSO_4$, and the solvent evaporated to give a viscous liquid. To remove all 2-bromo-2-methylpropionic acid byproduct (singlet at 1.89 ppm in ^{1}H NMR), the residue was stirred with hot water several times and again dissolved in diethyl ether. After drying and evaporation of the diethyl ether, the crude product was recrystallized from hexane to give the product as a white solid: 36 g (56%); mp 96.6 °C. ^{1}H NMR ($CDCl_3$): δ 1.33 (s, 3H, $-CH_3$), 1.89 (s, 12H, $-C(Br)-CH_3$), 4.43−4.41 (q, 4H, $-CH_2-$). ^{13}C NMR ($CDCl_3$): δ 17.78, 30.63, 46.56, 55.21, 65.97, 170.96, 178.57. IR (cm^{-1}): 2700−3200, 1736, 1694, 1289, 1178, 1105. Elemental Analysis: Calcd for $C_{13}H_{20}Br_2O_6$: C, 36.10; H, 4.64; Br, 36.90. Found: C, 36.95; H, 4.98; Br, 37.10.

Initiators (General Procedure). The hydoxyl-functionalized precursors (2 g) together with **3** (1.1 equiv with respect to OH groups) were dissolved in ca. 20 mL of dichloromethane. Then 4-(dimethylamino)pyridinum 4-toluenesulfonate (DPTS, 0.1 equiv) and dicyclohexyl carbodiimide (DCC, 1.5 equiv) were added in that order, and the solution was stirred at room temperature overnight. The solution was filtered to remove

Scheme 1

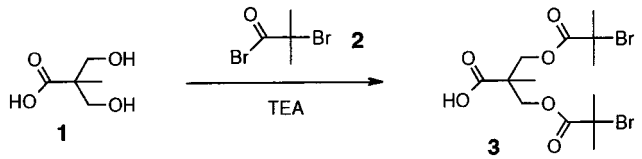

the urea byproduct and the product purified by flash chromatography (silica gel, hexane/ethyl acetate 4:1).

2-Arm Initiator ***8***. Yield 70% (solid); mp 60.6 °C. ^{1}H NMR ($CDCl_3$): δ 1.33 (s, 3H, $-CH_3$), 1.83 (s, 12H, $-C(Br)-CH_3$), 4.43−4.41 (q, 4H, $-CH_2-$), 5.16 (s, 2H, $Ar-CH_2-$), 7.31 (s, 5H, ArH). ^{13}C NMR ($CDCl_3$): δ 17.89, 30.59, 46.74, 55.33, 66.33, 67.12, 128.29, 128.46, 128.66, 135.36, 170.94, 172.19. IR (cm^{-1}): 2800−3100, 1736, 1478, 1300, 1176.

4-Arm Initiator ***9***. Yield 74% (viscous liquid). ^{1}H NMR ($CDCl_3$): δ 1.22 (s, 6H, $-CH_3$), 1.27 (s, 3H, $-CH_3$), 1.88 (s, 32H, $-C(Br)-CH_3$), 4.26 (m, 12H, $-CH_2-$), 5.14 (s, 2H, $Ar-CH_2$), 7.32 (s, 5H, ArH). ^{13}C NMR ($CDCl_3$): δ 17.76, 30.63, 46.74, 55.33, 65.95, 66.08, 67.23, 128.48, 128.58, 128.71, 135.32, 170.82, 171.60, 171.89. IR (cm^{-1}): 2800−3100, 1735, 1465, 1263, 1144.

6-Arm Initiator ***10***. Yield 90% (solid); T_g 30.3 °C. ^{1}H NMR ($CDCl_3$): δ 1.47 (s, 9H, $-CH_3$), 1.92 (s, 36H, $-C(Br)-CH_3$), 2.13 (s, 3H, Ar_3-C-CH_3), 4.47 (q, 12H, $-CH_2-$), 7.05 (dd, 12 H, ArH). ^{13}C NMR ($CDCl_3$): δ 17.91, 30.7, 47.11, 51.69, 55.21, 66.32, 120.81, 129.78, 146.38, 148.58, 171.02, 171.14. IR (cm^{-1}): 2800−3100, 1742, 1515, 1463, 1284, 1221, 1168, 1105. Elemental Analysis: Calcd for $C_{59}H_{72}Br_6O_{18}$: C, 45.76; H, 4.69; Br, 30.96. Found: C, 45.38; H, 5.01; Br, 30.99.

12-Arm Initiator ***11***. Yield 43% (solid); T_g 23.0 °C. ^{1}H NMR ($CDCl_3$): δ 1.33 (s, 18H, $-CH_3$), 1.41 (s, 9H, $-CH_3$), 1.87 (s, 72H, $-C(Br)-CH_3$), 2.14 (3H, Ar_3-C-CH_3), 4.37 (q, 36H, $-CH_2-$), 7.03 (dd, 12 H, ArH). ^{13}C NMR ($CDCl_3$): δ 17.84, 17.95, 30.62, 46.85, 47.02, 55.33, 66.00, 120.70, 129.82, 146.37, 148.51, 170.72, 170.87, 171.67. IR (cm^{-1}): 2800−3000, 1739, 1475, 1269, 1170, 1108. Elemental Analysis: Calcd for $C_{113}H_{150}Br_{12}O_{42}$: C, 45.35; H, 4.74; Br, 30.80. Found: C, 46.03; H, 4.89; Br, 31.18.

Polymerizations. The polymerization of freshly vacuum-distilled methyl methacrylate (MMA) was performed in bulk. The respective initiators and the catalyst, bis(triphenylphosphine)nickel dibromide (10−30% with respect to bromine functionality), were first weighed into a flame-dried round-bottom flask equipped with a three-way stopcock. Several cycles involving evacuation and subsequent argon purging were conducted to remove most of the dissolved oxygen. Finally, the purified and degassed MMA monomer was added under argon using a syringe and the mixture heated to 90 °C until the contents of the flask completely solidified (2−4 h). The polymer was then dissolved in THF and precipitated by

Scheme 2

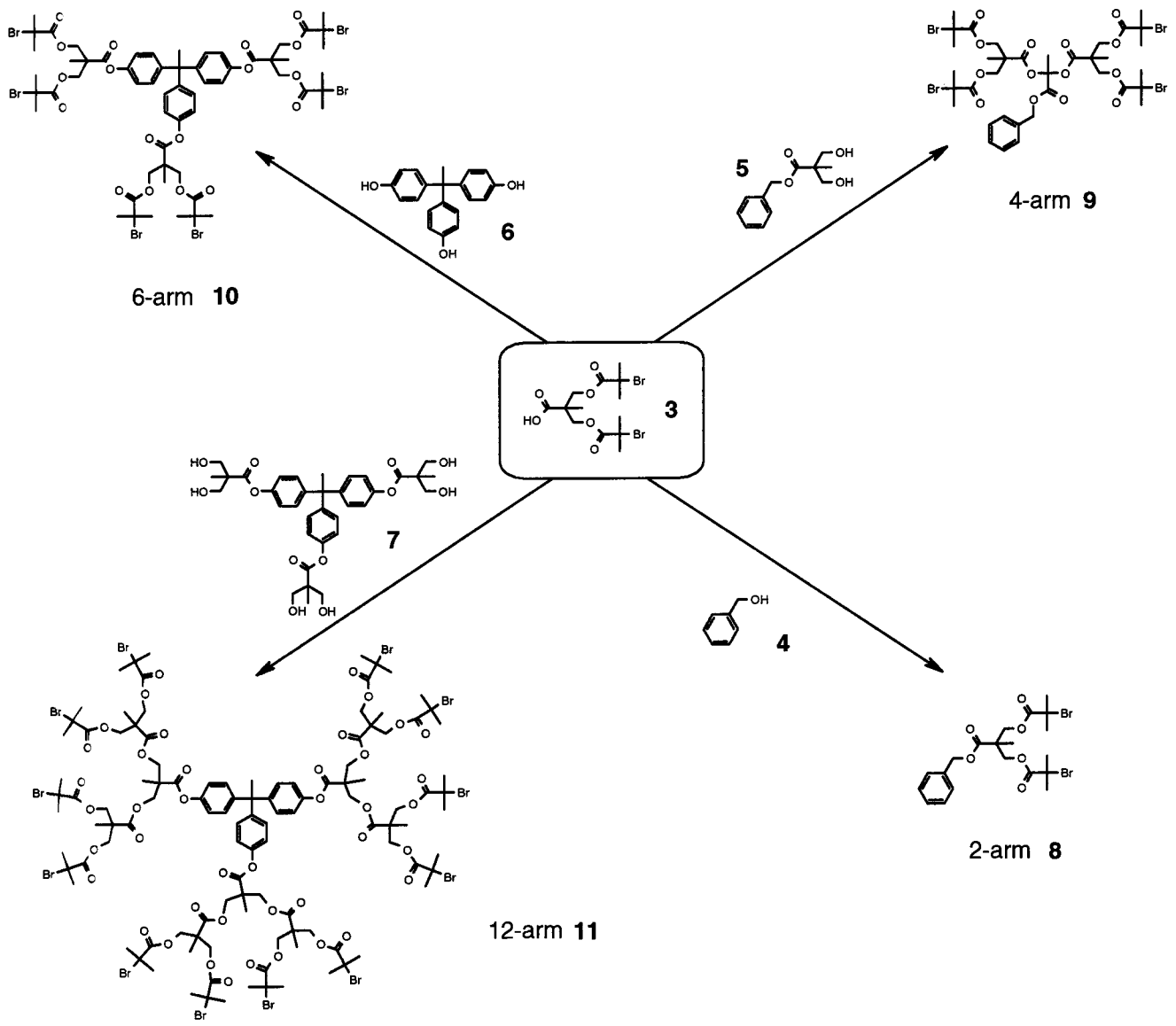

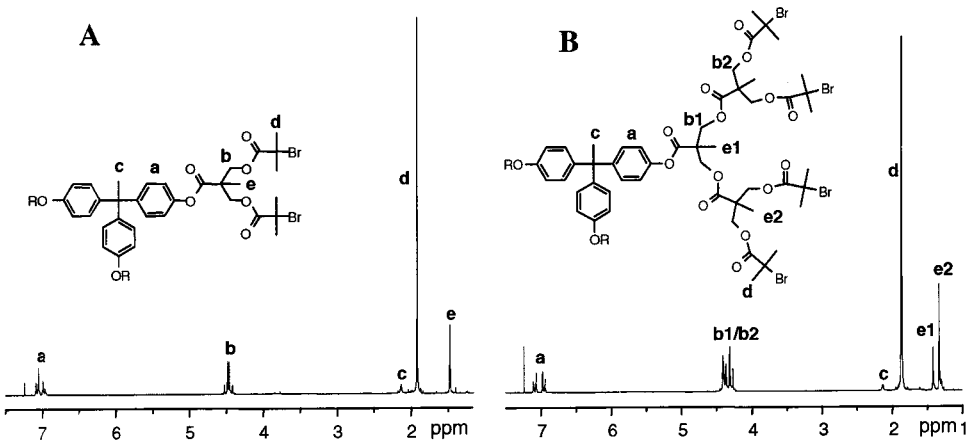

Figure 1. ^{1}H NMR spectra of the dendritic 6- and 12-arm initiators.

addition to methanol. The copolymerizations were carried out similarly in freshly distilled THF (monomer/THF ca. 1:2).

Results and Discussion

Initiators. All initiators for the ATRP studies were prepared by esterfication of hydroxy-functionalized precursors with the 2-bromo-2-methylpropionyl-functionalized building block **3** using dicyclohexyl carbodiimide (DCC) and 4-(dimethylamino)pyridinium 4-toluenesulfonate (DPTS)[45] according to Scheme 2. Whereas the linear or 1-arm initiator is represented by the benzyl ester of 2-bromo-2-methylpropionic acid, the higher functionality initiators employ branched and dendritic structures derived from 2,2-bis(hydroxymethyl)propionic acid, **1** (bis-MPA). To simplify the synthesis of higher generation initiators, the carboxy functionalized 2-arm precursor **3** was synthesized from bis-MPA (**1**) and 2-bromo-2-methylpropionyl bromide (**2**) using triethylamine as a proton scavenger (Scheme 1). Using this building block, initiators with larger numbers of arms can be prepared in a straightforward fashion (Scheme 2).

The benzyl ester protected AB_2 building block **8** was produced in 70% yield by esterfication of the acid **3** with benzyl alcohol. To synthesize the 4-arm initiator **9**, i.e., a second generation bromo functional dendron of bis-MPA (the benzyl ester of bis-MPA), **5** was esterified with the bromo-functionalized building block **3** (74% yield). The 6-arm initiator **10** was prepared similarly using commercially available 1,1,1-tris(*p*-hydroxyphenyl)ethane (THPE), **6**, as a trifunctional hydroxylated core. This initiator, prepared in 69% yield, represents the first generation bromo-functionalized dendron derived from the trifunctional core. The corresponding 12-arm initiator **11**, i.e., the second generation dendron, was prepared similarly in 62% yield using the carboxy-functionalized AB_2 building block and the 6-arm hydroxyl-functionalized precursor **7**, which was prepared according to literature procedures.[46−48] Spectral data of all initiators are in accordance with the suggested structures. Figure 1 shows the ^{1}H NMR spectra of both the 6- and 12-arm initiators as representative examples. Beside the signals of the aromatic core (a and c), both spectra show the signals of the dendritic branches of the different generations (b and e) as well as the characteristic signal of the methyl groups attached to the activated bromide (d) at 1.82 ppm. Interestingly, the signal for the methylene groups b appears as an AB quartet at 4.5 ppm in the 6-arm initiator and as two such AB multiplets (b1 and b2) in the 12-arm initiator representing first and second generations of these protons in the latter. The peak intensity ratios are in accordance with the theoretical number of initiator sites for each multiarm initiator. Elemental analyses were performed on representative examples such as the building block **3**, the 6-arm initiator **10**, and the 12-arm initiator **11**. The data obtained are in accordance with the theoretical composition.

Homopolymerization. The polymerization of freshly vacuum-distilled methyl methacrylate (MMA) was performed in bulk at 90 °C using bis(triphenylphosphine)-nickel(II) bromide as a catalyst.[49] All of the initiators were readily soluble in this monomer, and the polymerizations proceeded smoothly causing the contents of the flask to ultimately solidify.

Three target molecular weights, e.g., 10 000, 28 000, and 100 000 g/mol, calculated from the monomer-to-initiator ratio, were selected for each polymer. The measured number-average molecular weights ($\bar{M}_n$) of the respective polymers were determined both from ^{1}H NMR integration and from size exclusion chromatography (SEC). However, since the SEC analyses are based on calibration with linear polystyrene standards, the values of the molecular weights are questionable. This technique often underestimates the molecular weight of branched and hyperbranched polymers, since the shapes of these polymers are more globular in comparison with linear random coil polymers.[50] In this regard, we have previously observed an increasing discrepancy between the molecular weights determined by the SEC and ^{1}H NMR for starlike PCL derivatives as the number of arms increases.[12] This has also been reported by Sawamoto for an 8-arm star PMMA.[43] Molecular weights of starlike polymers determined using solely SEC with linear calibrants should therefore be viewed with some caution.

Accurate $\bar{M}_n$ values can be obtained by ^{1}H NMR analyses of the lower molecular weight polymers by calculating the ratio of the integrated peak areas of the methyl ester side chains present in the PMMA polymers (g in Figure 4) to those of the aromatic protons of the initiator core (a). As can be seen in Table 1, the $\bar{M}_n$ values measured by NMR are in fairly good agreement with the predicted values derived from the monomer/initiator ratio for all of the polymers described when the monomer conversion is >90%. This suggests that there are no significant differences in reactivity of the initiator arms in the ATRP of MMA even for multiarm initiators.

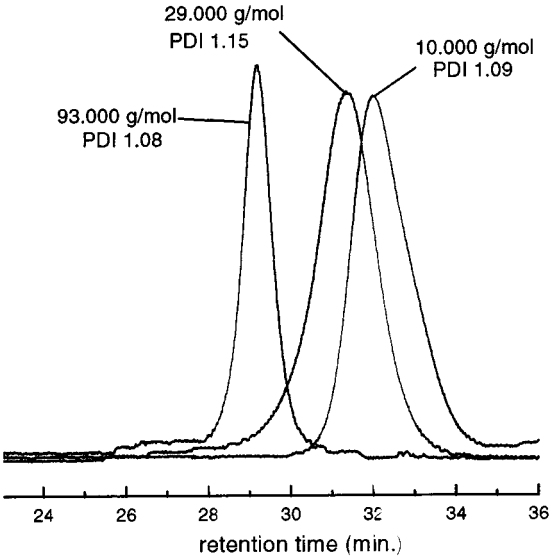

Figure 2. SEC traces of 6-arm PMMA samples of different molecular weight (PDI = polydispersity index).

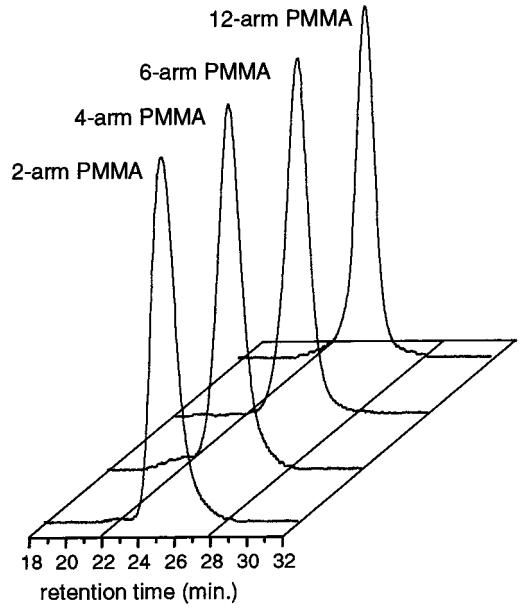

Figure 3. SEC traces of multiarm starlike PMMAs of comparable molecular weight (26 000−28 000 g/mol) containing varying numbers of arms.

For a series of polymers of constant overall molecular weight, the average degree of polymerization (DP) per arm decreases with increases with the number of initiating arms, i.e., with the degree of branching. For the target 28 000 g/mol series, it varies from 130 per arm for the 2-arm to 22 per arm for the 12-arm branched PMMA polymer. In addition, we also prepared several different polymer molecular weights from each initiator, i.e., polymers containing a constant number of arms but changing DP. In the case of the 6-arm polymers, for example, the DP per arm was varied from 17 (10 000 g/mol polymer) to 155 (93 000 g/mol) per arm.

Although the results from the SEC analyses may not reflect the true molecular masses for more highly branched polymers, this technique is still a convenient method for determining the polydispersity of the synthesized star polymers. In accordance with the proposed living/controlled character of ATRP process, low polydispersities were measured for all homopolymers (1.08−1.16). Even for the 6- and 12-arm polymers, the polydispersities are remarkably low and independent of the molecular weight of the polymer. Moreover, the SEC peaks are all reasonably symmetrical (Figures 2 and 3) with no evidence of a high molecular weight tail that might be associated with intermolecular radical−radical coupling. However, the SEC data do not rule out the possibility of intramolecular coupling (cyclization), particularly at high molecular weights.

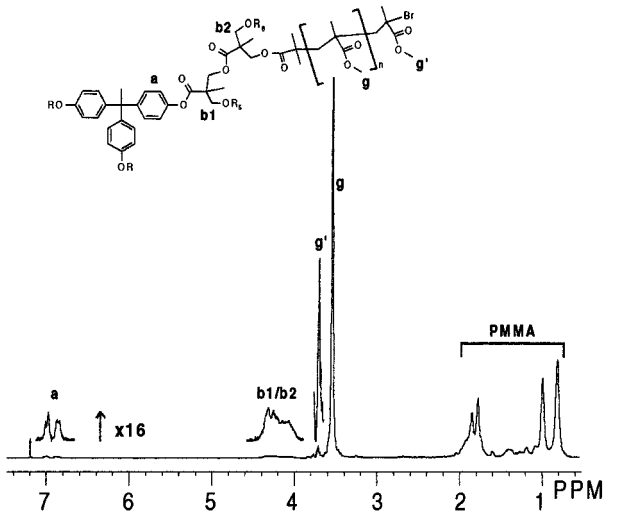

Figure 4. ^{1}H NMR spectrum of the starlike PMMA derived from the dendritic 12-arm initiator.

Table 1. Polymer Characteristics of Starlike Poly(methyl methacrylate)s. Target Molecular Weights Are 10 000, 28 000, and 100 000 g/mol for the 2-, 4-, and 6-Arm Polymers and 28 000 and 100 000 g/mol for the 12-Arm Polymer, Respectively. Accurate Molecular Weights and Numbers of End Groups Are Not Available for High Molecular Weight Samples from ^{1}H NMR Analysis Due to Low Concentration of End Groups

polymer	$\bar{M}_n$(SEC), g/mol[a]	$\bar{M}_n$(^{1}H NMR), g/mol[b]	$\bar{M}_n/\bar{M}_w$	no. of end groups[c]
2-arm	6 000	11 000	1.14	1.9
	15 000	26 000	1.16	2.4
	68 000	n/a	1.2	n/a
4-arm	6 000	12 500	1.13	3.7
	14 000	28 200	1.16	4.4
	74 000	n/a	1.18	n/a
6-arm	6 000	10 000	1.09	5.1
	15 000	28 900	1.15	5.2
	78 000	n/a	1.08	n/a
12-arm	13 000	26 500	1.08	10.5
	55 000	n/a	1.14	n/a

[a] GPC calibrated to polystyrene standards. [b] Calculated from the ratio of initiator aromatic protons to methyl ester groups in the polymer. [c] Calculated from the respective NMR peaks.

To verify that all arms of the initiator reacted in the polymerization, the ^{1}H and ^{13}C NMR spectra were carefully analyzed. Figure 4 shows the ^{1}H NMR spectrum of the polymer derived from the 12-arm initiator. By comparison with the spectrum of the initiator **11** (Figure 1B), the peaks centered at 6.9 and 4.3 ppm (a and b in Figure 4) in the polymer can be assigned to the initiator core of the starlike macromolecule. Unfortunately, the terminal methyl groups of the initiator (d in Figure 1B) are not useful in analyzing whether polymerization has occurred from all arms of the initiator, since the intense proton signals of the growing polymer main chain overlap this resonance in the polymer (0.5−2 ppm). In the case of the 6-arm system, however, the signals of the bis-MPA methylene groups

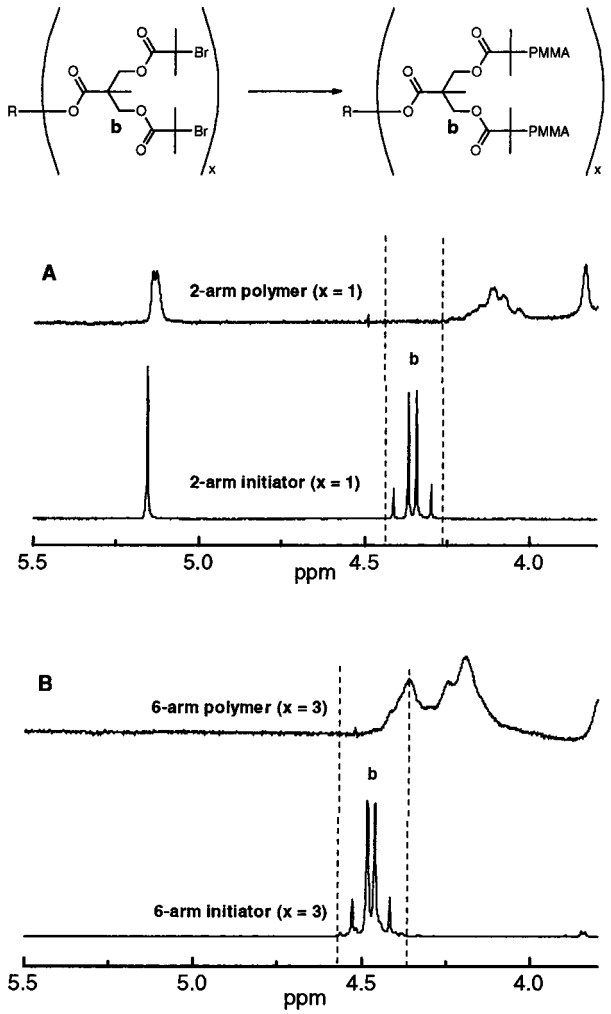

Figure 5. ^{1}H NMR spectral expansion of the region of the methylene protons before and after polymerization for the 2- (A) and 6-arm (B) derivatives.

(b Figure 1A) of the initiator are useful. Since the 2-arm polymer itself represents one dendritic unit of the 6-arm polymer, it can be used as a model to study the effect on the chemical shift of the methylene groups caused by polymerization. Figure 5A shows an expansion of the methylene region of the spectrum for the 2-arm initiator **8** and the PMMA polymer thus derived. The AB multiplet centered around 4.3 ppm, which can be assigned to the methylene groups in the initiator, is broadened substantially and shifted upfield to about 4.1 ppm in the corresponding polymer spectrum. A similar upfield shift is observed for the 6-arm system. The fact that no signal can be detected at the original position of these protons in the polymer spectrum, even upon expansion, strongly suggests that all arms have initiated polymerization. Similar conclusions are drawn from the ^{1}H NMR spectra of the 6-arm initiator and polymer. Additional evidence for initiation from all arms of the 6-arm derivative is apparent from the ^{13}C NMR spectra of the starlike polymers where no residual carbon signal is observed around 67 ppm in the 6-arm polymer spectrum. Signals are observed in this region for the methylene carbons of the initiator, and polymerization also causes a significant upfield shift of these carbon resonances. However, it should be noted that this approach provides only tentative evidence for the initiation efficiency since the chemical shifts of residual initiator arms could change due to the proximity of polymer chains.

Extension of this analytical approach to the 12-arm derivatives is more difficult since the initiator contains both first and second generation methylene protons (b1/b2 in Figures 1 and 4) overlapping into a combined signal centered at about 4.3 ppm. The 4-arm polymer represents one dendritic segment of the 12-arm polymer and is therefore an appropriate model for study of the changes in the ^{1}H NMR chemical shifts upon polymerization. Although these signals appear as overlapping AB multiplets centered around 4.3 ppm in both the first and second generation initiators, growth of the polymer chains causes signal broadening and an upfield shift in the second generation methylene groups to about 4.1 ppm. Since the chemical shift of the outer methylene units should be most strongly affected by the proximate growing polymer chain, a residual signal from the inner core methylene groups around 4.2 ppm might be anticipated and is observed in the polymer. Because of the broadening of the respective signals upon polymerization, a firm conclusion regarding whether all arms initiate polymerization in the 12-arm system cannot be drawn.

In addition to the core initiator unit, the terminal end groups of the starlike polymers can be detected in the ^{1}H NMR spectra. For example, in the 12-arm polymer a small singlet at 3.7 ppm (g′) appears near the strong signal for the methoxycarbonyl groups of the MMA repeat units at 3.5 ppm (g, Figure 4). Consistent with the assignments of Sawamoto[33,51] and Teyssié,[32] this singlet is attributed to the methyl ester of the terminal bromo-functionalized monomer unit. Similar signals are observed for the 2-, 4-, and 6-arm polymers. From the peak area ratio a/g′ (Figure 4, 12-arm polymer), the number of end groups per star polymer were calculated for the 10 000 and 28 000 g/mol polymers (Table 1). The numbers for the 2-, 4-, and 6-arm polymers match reasonably well the theoretical number of polymer arms, irrespective of the molecular weight. Taking into account the error inherent in the integration of the small peak g′, due to overlapping signals (10−20%), these data provide additional evidence that polymerization has occurred on all arms of the initiators and also indicate that intramolecular radical coupling (cyclization), if it happens at all, occurs infrequently since this would result in a decrease in the number of functionalized end groups. In the case of the 12-arm polymer, we observed that the number of halogenated end groups calculated from the ^{1}H NMR spectra is sometimes lower than the theoretical value, and the ratio varies as a function of the polymerization conditions. To provide more information on whether this effect is related to the presence of unreacted arms remaining on the initiator or thermal dehalogenation or intramolecular radical−radical coupling (cyclization), we are currently investigating polymers derived from deuterated monomer (MMA-d_5; the methoxycarbonyl substituent is undeuterated). Preliminary results on the deuterated polymers indicate that the initiation is sometimes incomplete; i.e., the number of arms varies between 10 and 12 for the 12-arm initiator. The reasons for the incomplete initiation and the impact of varying polymerization conditions are currently under investigation and will be discussed in detail in a future paper. An initiator efficiency of 0.75 under similar polymerization conditions has been reported for linear initiators.[49]

Table 2. Polymer Characteristics of Starlike Poly(methyl methacrylate-*co*-hydroxyethyl methacrylate)s. Target Molecular Weight Is 5000 g/mol Including the Initiator Core

polymer[a]	$\bar{M}_n$(^{1}H NMR), g/mol[b]	$\bar{M}_n$(SEC), g/mol[c]	$\bar{M}_n/\bar{M}_w$	HEMA in polymer (mol %)
1-arm 5%	4300	3400	1.20	3
1-arm 10%	4800	3800	1.33	9
2-arm 5%	4000 (4700)	3300	1.25	9
2-arm 10%	4800 (5500)	4900	1.22	13
2-arm 20%	3400 (3900)	4700	1.33	25
4-arm 5%	4200 (5100)	5700	1.26	10
4-arm 10%	4300 (5200)	6600	1.26	16
4-arm 20%	4200 (5100)	6500	1.24	21
6-arm 5%	3300 (4800)	5000	1.34	8
6-arm 10%	3500 (5000)	5000	1.27	12
6-arm 20%	4200 (5700)	7500	1.25	19

[a] Number refers to the percentage of HEMA in the monomer feed. [b] Calculated from the ratio of initiator aromatic protons to the MMA methyl ester and HEMA methylene groups of the monomer units measured from ^{1}H NMR of the polymer. Values in parentheses refer to the molecular weight of the polymer plus the molecular weight of the initiator (see text).

Copolymerization. To facilitate the interaction of the branched porogen macromolecules with SSQ matrix materials in the formation of organic−inorganic hybrids, random copolymers containing MMA and varying amounts of hydroxyethyl methacrylate (HEMA) were prepared using the dendritic initiators in a solution (THF) polymerization. On the basis of the earlier results from PCL hybrids, a relatively low polymer molecular weight of 5000 g/mol was targeted.[38] As can be seen in Table 2, the number-average molecular weights determined by ^{1}H NMR analyses of all copolymers are slightly below the target molecular weight. However, this measured value considers only the polymer portion of the molecule, whereas SEC surveys the whole molecule. Unlike in the high molecular weight homopolymers, the contribution of the initiator core to the overall molecular weight is significant in the case of the lower molecular weight copolymers. The calculated molecular weights, including the initiator core, are given in parentheses in Table 2. For reasons discussed earlier, the direct comparisons between the NMR and SEC molecular weights must be viewed with some caution.

The polydispersities of MMA/HEMA copolymers are somewhat higher than for the MMA homopolymers. This can be attributed in part to the protic side chain functionality of the HEMA, favoring termination and chain transfer reactions. Fortunately, the extent of these side reactions is low, and the polydispersities are still reasonably low. An obvious dependency of copolymer polydispersity on the amount of HEMA in the comonomer feed was not observed. In general, it should be acknowledged that control of molecular weights, polydispersities, and conversions in the HEMA-containing copolymers is more complex than with MMA homopolymers. This has been also reported by Matyjaszewski for HEMA homopolymers prepared in solution.[52]

The incorporation of HEMA in the copolymer is confirmed by ^{1}H NMR analysis. Figure 6a−c shows the spectra of the 2-arm copolymers containing different concentrations of HEMA (nominally 5%, 10%, and 20%, respectively, based on the monomer feed). The composition of copolymers tracks the HEMA monomer feed ratio in the polymerization solution as indicated by the increase of the two characteristic HEMA side chain resonances around 3.8 and 4.1 ppm (a and b in Figure 6C) relative to the methoxy signal of the MMA (g in Figure 6C). Integration of the respective peak areas was used to generate the data shown in Table 2. The error due to overlapping signals, in particular for more highly branched initiators (compare Figure 4) and/or lower HEMA concentrations, is estimated to be ±2−3%. Taking this into account, the measured values are reasonably close to the monomer feed composition.

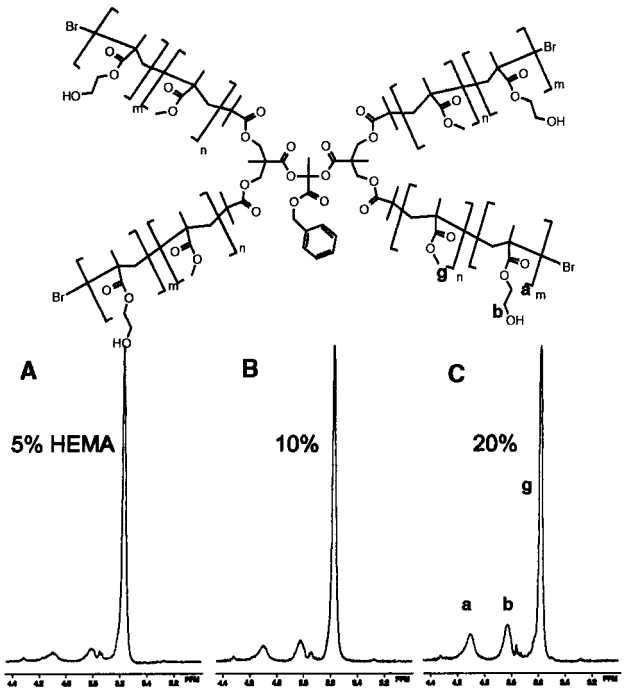

Figure 6. ^{1}H NMR spectra of 4-arm copolymers containing increasing amounts of HEMA (5% (A), 10% (B), 20% (C)).

Formation of Thin-Film Nanofoams. To investigate the appliciability of the star-branched methacrylate homo- and copolymers as pore generators (porogens) in the formation of nanoporous thin films, organic−inorganic hybrids were prepared following a general procedure. Solutions of the polymers (30% w/w) and methylsilsesquioxane (30% w/w; $\bar{M}_n \sim 1000$ g/mol) in propylene glycol methyl ether acetate (PM-acetate) were mixed in the desired ratio (20 wt % of polymer relative to MSSQ). This solution was then spin-coated on a silicon wafer and the matrix cured by first heating to 250 °C (5 °C/min) to initiate film vitrification. Subsequently, the films were heated to 450 °C to decompose the polymer. TGA analysis of the homo- and copolymers indicates the complete decomposition of the porogen under these conditions. Figure 7 shows the TGA traces of the linear copolymer samples. For the samples with varying amounts of HEMA, an initial weight loss between 250 and 280 °C is detected, the magnitude of which corresponds reasonably well to the amount of HEMA in the copolymer. Similar results were observed for the star-branched derivatives.

Preliminary results on the formation of organic−inorganic hybrids show that the starlike MMA homopolymers are prone to macroscopic phase separation upon curing. The thermal curing of the spin-coated films initiated macroscopic phase separation prior to the decomposition of the pore generators, resulting in optically opaque films. This can be rationalized by the limited miscibility between the PMMA and the vitrifying SSQ matrix under these conditions, an observation which is common for many polymer blends. Diffusion drives the phase separation into larger domains before the matrix is completely vitrified, effecting the optical

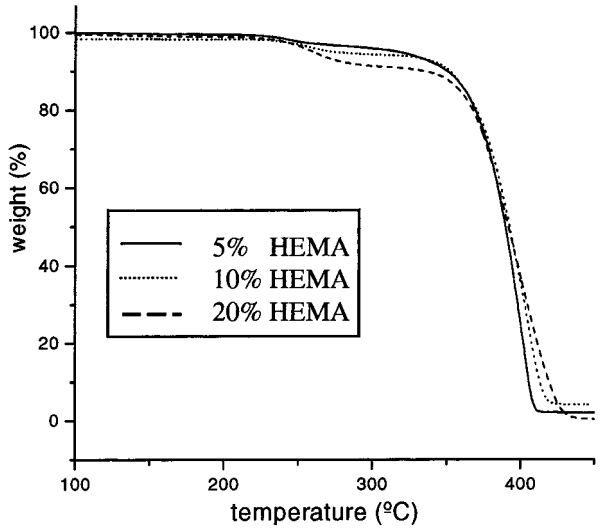

Figure 7. Thermal gravimetric analysis (TGA) of linear (1-arm, see Table 2) poly(MMA-*co*-HEMA) with varying amounts of HEMA. TGAs were performed under nitrogen at a heating rate of 2 °C/min.

transparency of the film. However, in the case of the HEMA-containing copolymers the phase separation is apparently mediated by the interaction of the hydroxy substituents with the MSSQ matrix. As a result, we obtained optically clear films from these polymer blends upon curing, a result consistent with either polymer miscibility or phase separation on a nanoscopic rather than micro- or macroscopic scale. The use of porogens with a starlike structure allows higher loading levels and the use of higher molecular weight samples relative to linear analogues before macroscopic phase separation (cloudy films) occurs upon vitrification. IR spectroscopy provides a convenient tool for monitoring the hybrid films during thermal curing. A carbonyl band (1720 cm^{-1}) clearly indicates the presence of the polymer in the hybrid film that had been cured to 250 °C, a temperature high enough to initiate matrix vitrification. After subsequent thermal decomposition of the polymer (430 °C), this band disappears and the film remains optically clear. To determine whether this process produced a foamed film with voids in the nanometer size range, TEM micrographs of the films were obtained. A representative image of the film obtained by curing the hybrid formed from MSSQ and the 6-arm copolymer (10% HEMA; 20 wt %) is shown in Figure 8. This image clearly shows voids (light) produced in the SSQ matrix (dark) with an average pore size of about 10 nm. The foamed morphology of the film was also confirmed by the significant decrease in the refractive index (633 nm) in the film after decomposition of the polymer ($n_{initial} \sim 1.4$; $n_{cured} \sim 1.3$). The measured dielectric constant (10 kHz) of the film was also considerably lower (2.2) than that of the densified MSSQ matrix (2.80).

These preliminary results indicate that the starlike methacrylate copolymers which are easily prepared by controlled radical polymerization techniques constitute novel and promising materials for the preparation of nanoporous, low dielectric constant films. The porous morphology of the organosilicate films is stable to temperatures in excess of 400 °C, a current requirement for on-chip insulator applications. Further investigations of the role of the chain branching and copolymer composition on the final porous film morphologies and dielectric constants are in progress.

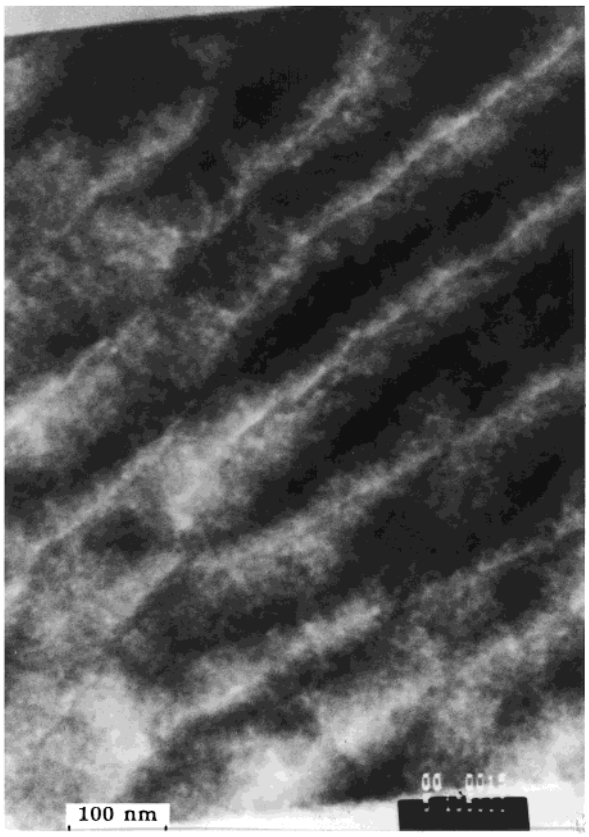

Figure 8. TEM image of a nanoporous thin film derived from a 6-arm copolymer (10% HEMA, see Table 2; 20 wt % polymer).

Conclusions

In conclusion, some novel poly(methyl methacrylate)s with starlike architectures have been synthesized by controlled radical polymerization starting from dendritic 2-, 4-, 6-, and 12-arm multifunctional initiators. The initiators were obtained by coupling a bromo-functionalized first generation dendron of bis-MPA to hydroxyl-functionalized precursors. The use of the ATRP technique allows the synthesis of branched and star polymers with accurate control of molecular weight and polydispersity. The controlled free radical character of the ATRP polymerization is supported by the remarkably low polydispersities of the homopolymers and the close correspondence between the calculated and measured molecular weights. NMR studies on the polymers were consistent with initiation occurring from all initiator arms for the 2-, 4-, and 6-arm polymer. Preliminary studies on polymers derived from the 12-arm initiator indicate somewhat less efficient initiation, and polymers with 10−12 arms were obtained. In addition, starlike copolymers containing varying amounts of hydroxyethyl methacrylate have been synthesized. The polydispersities of the copolymers are slightly higher than for the homopolymers. Preliminary results show that these copolymers can be used to produce nanophase-separated inorganic/organic hybrids by templating the vitrification of methylsilsesquioxane, and nanoporous thin films are generated by subsequent thermal degradation of the organic polymer. These polymers are promising novel templating materials for the preparation of porous low dielectric constant films.

Acknowledgment. The authors gratefully acknowledge the NSF funded Center on Polymer Interfaces and Macromolecular Assemblies (CPIMA) under Award

DMR-9400354. Andreas Heise also acknowledges partial support from the Deutsche Forschungsgemeinschaft (DFG). The authors thank Steve McCartney of the Material Science Department at Virginia Tech for the TEM micrographs.

References and Notes

(1) Hawker, C. J.; Malmström, E. E.; Frank, C. W.; Kampf, J. P. *J. Am. Chem. Soc.* **1997**, *119*, 9903.
(2) Fréchet, J. M. J. *Science* **1994**, *263*, 1710.
(3) Fréchet, J. M. J.; Hawker, C. J. In *Synthesis and properties of dendrimers and hyperbranched polymers*; Fréchet, J. M. J., Hawker, C. J., Eds.; Pergamon: New York, 1996; pp 71−132.
(4) Devonport, W.; Hawker, C. J. *Polym. News* **1996**, *21*, 370.
(5) Trollsås, M.; Hedrick, J. L.; Mecerreyes, D.; Dubois, P.; Jérôme, R.; Ihre, H.; Hult, A. *Macromolecules* **1997**, *30*, 8508.
(6) Kim, S. H.; Han, Y.-K.; Ahn, K.-D.; Kim, Young Ha; Chang, T. *Macromol. Chem.* **1993**, *194*, 3229.
(7) Tian, D.; Dubois, P.; Jérôme, R.; Tessié, P. *Macromolecules* **1994**, *27*, 4134.
(8) Lambert, O.; Dumas, P.; Hurtrez, G.; Riess, G. *Macromol. Rapid Commun.* **1997**, *18*, 343−351.
(9) Trollsås, M.; Atthoff, B.; Claesson, H.; Hedrick, J. L. *Macromolecules* **1998**, *31*, 3439.
(10) Trollsås, M.; Hedrick, J. L. *Macromolecules* **1998**, *31*, 4390.
(11) Trollsås, M.; Hawker, C. J.; Remenar, J. F.; Hedrick, J. L.; Johansson, M.; Ihre, H.; Hult, A. *J. Polym. Sci., Chem. Ed.* **1998**, *36*, 2793.
(12) Atthoff, B.; Trollsås, M.; Claesson, H.; Hedrick, J. L. *Macromol. Chem. Phys.*, in press.
(13) Kricheldorf, H. R.; Stukenbrock, T. *Polymer* **1997**, *38*, 3373.
(14) Trollsås, M.; Hedrick, J. L.; Mecerreyes, D.; Dubois, P.; Jérôme, R. *Polym. Mater. Sci. Eng.* **1997**, *77*, 208.
(15) Trollsås, M.; Hedrick, J. L. *J. Am. Chem. Soc.* **1998**, *120*, 4644.
(16) Trollsås, M.; Claesson, H.; Atthoff, B.; Hedrick, J. L. *Angew. Chem.* **1998**, *37*, 3132.
(17) Georges, M. K.; Veregin, R. P. N.; Kazmaier, P. M.; Hamer, G. K. *Macromolecules* **1993**, *26*, 2987.
(18) Hawker, C. J. *J. Am. Chem. Soc.* **1994**, *116*, 11314.
(19) Keoshkerian, B.; Georges, M. K.; Boils-Boissier, D. *Macromolecules* **1995**, *28*, 6381.
(20) Hawker, C. J. *Acc. Chem. Res.* **1997**, *30*, 373.
(21) Hawker, C. J.; Fréchet, J. M. J.; Grubbs, R. B.; J. D. *J. Am. Chem. Soc.* **1995**, *117*, 10763.
(22) Benoit, D.; Grimaldi, S.; Finet, J. P.; Tordo, P.; Fontanille, M.; Gnanou, Y. *Polym. Prepr.* **1997**, *38*, 729.
(23) Puts, R. D.; Sogah, D. Y. *Macromolecules* **1996**, *29*, 3323.
(24) Kazmaier, P. M.; Daimon, K.; Georges, M. K.; Hamer, G. K.; Veregin, R. P. N. *Macromolecules* **1997**, *30*, 2228.
(25) Wang, J.-S.; Matyjaszewski, K. *Macromolecules* **1995**, *28*, 7901.
(26) Matyjaszewski, K. In *Controlled Radical Polymerization*; Matyjaszewski, K., Ed.; ACS Symposium Series No. 685; American Chemical Society: Washington, DC, 1998.
(27) Matyjaszewski, K. *Macromolecules* **1998**, *31*, 4710.
(28) Ando, T.; Kato, M.; Kamigaito, M.; Sawamoto, M. *Macromolecules* **1996**, *117*, 5614.
(29) Percec, V.; Barboiu, B.; Kim, H.-J. *J. Am. Chem. Soc.* **1998**, *120*, 305.
(30) Kato, M.; Kamigaito, M.; Sawamoto, M.; Higashimura, T. *Macromolecules* **1995**, *28*, 1721.
(31) Moineau, G.; Granel, C.; Dubois, P.; Jérôme, R.; Teyssié, P. *Macromolecules* **1998**, *31*, 542.
(32) Granel, C.; Dubois, P.; Jérôme, R.; Teyssié, P. *Macromolecules* **1996**, *29*, 8576.
(33) Uegaki, H.; Kotani, Y.; Kamigaito, M.; Sawamoto, M. *Macromolecules* **1997**, *30*, 2249.
(34) Chiefari, J.; Chong, Y. K.; Ercole, F.; Krstina, J.; Jeffery, J.; Le, T. P. T.; Mayadunne, R. T. A.; Meijs, G. F.; Moad, C. L.; Moad, G.; Rizzardo, E.; Thang, S. H. *Macromolecules* **1998**, *31*, 5559.
(35) Hedrick, J. L.; Carter, K. R.; Labadie, J. W.; Miller, R. D.; Volksen, W.; Hawker, C. J.; Yoon, D. Y.; Russel, T. P.; McGrath, J. E.; Briber, R. M. *Adv. Polym. Sci.* **1999**, *141*, 1.
(36) Hedrick, J. L.; Hawker, C. J.; Miller, R. D.; Twieg, R.; Srinivasan, S. A.; Trollsås, M. *Macromolecules* **1997**, *30*, 7607.
(37) Hedrick, J. L.; Cha, H. J.; Miller, R. D.; Yoon, D. Y. *Macromolecules* **1997**, *30*, 8512.
(38) Hedrick, J. L.; Miller, R. D.; Hawker, C. J.; Carter, K. R.; Volksen, W.; Yoon, D. Y.; Trollsås, M. *Adv. Mater.* **1998**, *10*.
(39) Heise, A.; Hedrick, J. L.; Trollsås, M.; Miller, R. D.; Frank, C. W. *Macromolecules* **1999**, *32*, 231.
(40) Heise, A.; Hedrick, J. L.; Trollsås, M.; Miller, R. D.; Frank, C. W. *Polym. Prepr.* **1998**, *39*, 627.
(41) Heise, A.; Hedrick, J. L.; Miller, R. D.; Frank, C. W. *J. Am. Chem. Soc.* **1999**, *121*, 8647.
(42) Angot, S.; Murthy, K. S.; Tanton, D.; Gnanou, Y. *Macromolecules* **1998**, *31*, 7218.
(43) Ueda, J.; Kamigaito, M.; Sawamoto, M. *Macromolecules* **1998**, *31*, 6762.
(44) Xia, J.; Zhang, X.; Matyjaszewski, K. *Macromolecules* **1999**, *32*, 4482.
(45) Moore, J. S.; Stupp, S. I. *Macromolecules* **1990**, *23*, 65.
(46) Ihre, H.; Hult, A. *Polym. Mater. Sci. Eng.* **1997**, *77*, 71.
(47) Ihre, H.; Hult, A.; Soderlind, E. *J. Am. Chem. Soc.* **1996**, *118*, 6388.
(48) Trollsås, M.; Hedrick, J. L.; Mecerreyes, D.; Dubois, P.; Jérôme, R.; Ihre, H.; Hult, A. *Macromolecules* **1998**, *31*, 2756.
(49) Moineau, G.; Minet, M.; Dubois, P.; Teyssié, P.; Senninger, T.; Jérôme, R. *Macromolecules* **1999**, *32*, 27.
(50) Grest, G. S.; Fetters, L. J.; Huang, J. S.; Richter, D. In *Advances in Chemical Physics*; Prigogine, I., Rice, S. A., Eds.; John Wiley & Sons: New York, 1996; Vol. XCIV, pp 67−163.
(51) Nishikawa, T.; Ando, T.; Kamigaito, M.; Sawamoto, M. *Macromolecules* **1997**, *30*, 2244.
(52) Beers, K. L.; Boo, S.; Matyjaszewski, K. *Polym. Mater. Sci. Eng.* **1998**, *79*, 407.

MA991091R